Focal Adhesion Kinase Promotes Hepatic Stellate Cell Activation by Regulating Plasma Membrane Localization of TGFβ Receptor 2

Yunru Chen,[1*] Qing Li,[1*] Kangsheng Tu,[1*] Yuanguo Wang,[1] Xianghu Wang,[1] Dandan Liu,[1] Chen Chen,[1*] Donglian Liu,[1**] Rendong Yang,[2] Wei Qiu ,[3] and Ningling Kang[1]

Transforming growth factor β (TGFβ) induces hepatic stellate cell (HSC) differentiation into tumor-promoting myofibroblast, although underlying mechanism remains incompletely understood. Focal adhesion kinase (FAK) is activated in response to TGFβ stimulation, so it transmits TGFβ stimulus to extracellular signal-regulated kinase and P38 mitogen-activated protein kinase signaling. However, it is unknown whether FAK can, in return, modulate TGFβ receptors. In this study, we tested whether FAK phosphorylated TGFβ receptor 2 (TGFβR2) and regulated TGFβR2 intracellular trafficking in HSCs. The FAKY397F mutant and PF-573,228 were used to inhibit the kinase activity of FAK, the TGFβR2 protein level was quantitated by immunoblotting, and HSC differentiation into myofibroblast was assessed by expression of HSC activation markers, alpha-smooth muscle actin, fibronectin, or connective tissue growth factor. We found that targeting FAK kinase activity suppressed the TGFβR2 protein level, TGFβ1-induced mothers against decapentaplegic homolog phosphorylation, and myofibroblastic activation of HSCs. At the molecular and cellular level, active FAK (phosphorylated FAK at tyrosine 397) bound to TGFβR2 and kept TGFβR2 at the peripheral plasma membrane of HSCs, and it induced TGFβR2 phosphorylation at tyrosine 336. In contrast, targeting FAK or mutating Y336 to F on TGFβR2 led to lysosomal sorting and degradation of TGFβR2. Using RNA sequencing, we identified that the transcripts of 764 TGFβ target genes were influenced by FAK inhibition, and that through FAK, TGFβ1 stimulated HSCs to produce a panel of tumor-promoting factors, including extracellular matrix remodeling proteins, growth factors and cytokines, and immune checkpoint molecule PD-L1. Functionally, targeting FAK inhibited tumor-promoting effects of HSCs *in vitro* and in a tumor implantation mouse model. *Conclusion:* FAK targets TGFβR2 to the plasma membrane and protects TGFβR2 from lysosome-mediated degradation, thereby promoting TGFβ-mediated HSC activation. FAK is a target for suppressing HSC activation and the hepatic tumor microenvironment. (*Hepatology Communications* 2020;4:268-283).

Transforming growth factor β (TGFβ) induces activation of hepatic stellate cells (HSCs) into tumor-promoting myofibroblasts by initiating a series of intracellular signaling events, including ligation of TGFβ receptor I (TGFβR1) and TGFβ receptor 2 (TGFβR2) at the plasma membrane, endocytosis of TGFβR1/TGFβR2 complexes, phosphorylation and nuclear translocation of mothers against decapentaplegic homolog (SMAD), and gene transcription in the nucleus.[1-3] TGFβ stimulates HSCs to

Abbreviations: ANOVA, analysis of variance; BAF, bafilomycin; CM, conditioned medium; coIP, coimmunoprecipitation; CTGF, connective tissue growth factor; DMSO, dimethyl sulfoxide; ERK, extracellular signal-regulated kinase; F, phenylalanine; FAK, focal adhesion kinase; FAKwt, wild-type FAK; FGF2, fibroblast growth factor 2; GAPDH, glyceraldehyde 3-phosphate dehydrogenase; H&E, hematoxylin and eosin staining; HA, hemagglutinin; HSC, hepatic stellate cell; IF, immunofluorescence; IGF-1, insulin growth factor-1; IP, immunoprecipitation; LAMP1, lysosome-associated membrane glycoprotein 1; MAPK, mitogen-activated protein kinase; MTS, 3-(4,5-dimethylthiazol-2-yl)-5-(3-carboxymethoxyphenyl)-2-(4-sulfophenyl)-2H-tetrazolium; PD-L1, programmed death-ligand 1; PepA, pepstatin A; p-FAK, phosphorylated FAK; PY, phosphorylated tyrosine; RNA-seq, RNA sequencing; shRNA, short hairpin RNA; SMAD, mothers against decapentaplegic homolog; TGFβ, transforming growth factor β; TGFβR1, transforming growth factor-beta receptor I; TGFβR2, transforming growth factor-beta receptor II; WB, western blot analysis; wt, wild type; Y, tyrosine; α-SMA, alpha-smooth muscle actin.

Received August 21, 2019; accepted November 3, 2019.
Additional Supporting Information may be found at onlinelibrary.wiley.com/doi/10.1002/hep4.1452/suppinfo.

express α-smooth muscle actin (α-SMA), fibronectin and connective tissue growth factor (CTGF), markers of HSC activation,[4,5] and paracrine factors that promote liver metastatic growth.[6] Understanding how TGFβ signaling events are regulated, such as how TGFβ receptors distribute and traffic in HSCs, will help identify targets to inhibit HSC activation and the metastasis-promoting liver microenvironment.

Focal adhesion kinase (FAK) is a 125-kDa nonreceptor tyrosine (Y) kinase. It consists of an N-terminal FERM domain, a middle kinase domain, and a C-terminal FAT domain.[7,8] Inactive FAK exists as an auto-inhibited monomer, and its autophosphorylation at Y397 creates a binding site for SH2 domain of Src, so that Src is recruited to induce phosphorylation of FAK at additional sites, leading to full activation of FAK kinase.[7,8] In addition, FAK functions as a protein scaffold for signal transduction, independent of its kinase-activity.[7,9] At focal adhesions and adherens junctions, FAK is pivotal for establishing cell/substrate and cell/cell adhesions important for cell migration.[10,11] At the downstream of plasma membrane receptors, such as integrins, receptor Y kinases, G-protein coupled receptors and cytokine receptors, FAK transmits extracellular stimuli to PI3K/Akt, extracellular signal-regulated kinase (ERK), Jun N-terminal kinase (JNK), and Rho-family small guanosine triphosphatase signaling, contributing to the fundamental cell biological processes, such as cell adhesion, migration, proliferation, and survival.[7,12-14] FAK is a therapeutic target of cancer.

FAK is also a therapeutic target for fibrotic diseases. Phosphorylation and the activity of FAK were upregulated in scleroderma dermal fibroblasts and fibroblasts of lung fibrosis patients.[15,16] It has been shown that at the downstream of platelet-derived growth factor and TGFβ receptors, FAK transmits signals to Akt, ERK, and p38 mitogen-activated protein kinase (MAPK) pathways that contribute to HSC activation and liver fibrosis.[13,17,18] However, it is unknown whether FAK in return modulates TGFβ receptors. Using FAKY397F mutant and PF-573,228 (PF228) targeting the kinase activity of FAK, we found that inactivation of FAK indeed reduced TGFβR2 protein level and HSC activation induced by TGFβ. Mechanistically, active FAK induced phosphorylation of TGFβR2 at Y 336 and led to plasma membrane localization of TGFβR2 of HSCs. In contrast, inhibition of FAK kinase activity or mutating Y336 to F on TGFβR2 led to rapid lysosomal sorting and degradation of TGFβR2. In addition, RNA sequencing and biochemical and tumor implantation studies demonstrated that through FAK, TGFβ1 stimulated HSCs to produce a panel of tumor-promoting factors,

*Current address: First Affiliated Hospital of Xi'an Jiaotong University, Xi'an, Shanxi, P. R. China.
**Current address: Sixth Affiliated Hospital of Guangzhou Medical University, Qingyuan, Guangdong, P. R. China.
Financial Support: National Institutes of Health (R01 CA160069 to N.K.; R01 CA197128 to Q.W.); China Scholarship Council (to Q.L. and C.C.); and Y.C. and D.L. were funded by their hospitals in P. R. China.
RNA sequencing data: Gene Expression Omnibus GSE127964.
© 2019 The Authors. Hepatology Communications published by Wiley Periodicals, Inc., on behalf of the American Association for the Study of Liver Diseases. This is an open access article under the terms of the Creative Commons Attribution-NonCommercial-NoDerivs License, which permits use and distribution in any medium, provided the original work is properly cited, the use is non-commercial and no modifications or adaptations are made.
View this article online at wileyonlinelibrary.com.
DOI 10.1002/hep4.1452

Potential conflict of interest: Nothing to report.

ARTICLE INFORMATION:

From the [1]Tumor Microenvironment and Metastasis; [2]Computational Cancer Genomics, Hormel Institute, University of Minnesota, Austin, MN; [3]Department of Surgery and Cancer Biology, Loyola University Chicago Stritch School of Medicine, Maywood, IL.

ADDRESS CORRESPONDENCE AND REPRINT REQUESTS TO:

Ningling Kang, Ph.D.
Tumor Microenvironment and Metastasis
Hormel Institute, University of Minnesota
801 16th Ave NE
Austin, MN 55912
E-mail: nkang@umn.edu
Tel.: +1-507-437-9680

including programmed death ligand 1 (PD-L1), insulin growth factor-1 (IGF-1) and fibroblast growth factor-2 (FGF-2), and that targeting FAK inhibited paracrine tumor–promoting effects of HSCs *in vitro* and in mice. Thus, FAK promotes activation of HSCs into tumor-promoting myofibroblasts by targeting TGFβR2 to the plasma membrane and protecting it from lysosome-mediated degradation.

Materials and Methods

CELL LINES

Human primary HSCs were bought from ScienCell Research laboratories (5300; Carlsbad, CA) and cultured with Dulbecco's modified Eagle's medium supplemented with 10% fetal bovine serum, penicillin, and streptomycin. Cells with passage between 5 and 8 were used for experiments. HT29 human colorectal cancer cells were purchased from ATCC (HTB38; Manassas, VA) and authenticated by Genetica by short tandem repeat DNA profiling method. Cells were routinely monitored for mycoplasma infection using a MycoAlert detection kit (Lonza Group AG, Basel, Switzerland) and were free of infection.

ANTIBODIES AND REAGENTS

Antibodies, inhibitors, and plasmids containing FAK short hairpin RNA (shRNA) are found in the Supporting Information.

SITE-DIRECTED MUTAGENESIS AND VIRAL TRANSDUCTION OF CELLS

Wild-type chicken FAK complementary DNA[19] was inserted into a retroviral pMMP vector by standard polymerase chain reaction (PCR)-based subcloning techniques, and FLAG tag was added. pMMP-TGFβR2wt-hemagglutinin (HA) and pMMP-TGFβR1wt-FLAG were created in one of our previous studies.[4] Using a Q5 Site-Directed Mutagenesis Kit (E0054; NEB, Ipswich, MA), Y to phenylalanine (F) mutants pMMP-FLAG-chFAKY397F, pMMP-TβRIIY336F-HA, pMMP-TβRIIY259F-HA, and pMMP-TβRIIY424F-HA were created. All constructs were confirmed by sequencing and protein expression analysis. Lentiviruses and retroviruses were generated by cotransfecting 293T cells with multiple plasmids, as described previously.[20-22] Methods for viral transduction of HSCs are found in the Supporting Information.

IMMUNOFLUORESCENCE, WESTERN BLOT ANALYSIS, IMMUNOPRECIPITATION, CO-IMMUNOPRECIPITATION, AND DATA QUANTIFICATION

Immunofluorescence (IF) with HSCs or mouse tissue sections was done as described.[20,21] For western blot analysis (WB), protein samples were prepared by lysing cells or mouse tissues with radio immunoprecipitation assay buffer supplemented with phenylmethylsulfonyl fluoride, protease inhibitor cocktails (88266; Thermo Fisher Scientific, Waltham, MA), Na_3VO_4, and NaF. To study TGFβR2/FAK interactions in HSCs or Y phosphorylation on TGFβR2-HA, cells were lysed with buffer containing 0.5% Nonidet P40 (NP-40) for immunoprecipitation (IP).[4,5,22] Details regarding IF, WB, IP, and data analysis are found in the Supporting Information.

ANALYSIS OF CELL SURFACE TGFβR2 BY BIOTINYLATION AND TGFβR2 DEGRADATION

HSCs on cell culture dishes were first incubated with biotin (EZ-Link Sulfo-NHS-Biotin, 21217; Thermo Fisher Scientific) at 4°C for 30 minutes to label cell surface proteins. After free biotins were removed, cells were lysed with buffer containing 0.5% NP-40 and streptavidin agarose beads (S1638; Sigma-Aldrich, St. Louis, MO) were added into the lysates to pull down biotinylated cell surface proteins.[5] After protein electrophoresis, biotinylated TGFβR2 (cell surface TGFβR2) was quantitated by WB using anti-TGFβR2.[5,22] The half-life of wild-type TGFβR2 and TGFβR2 mutant in HSCs was analyzed by a method we used previously.[4] Details are found in the Supporting Information.

RNA SEQUENCING

An RNeasy Plus Mini Kit was used to isolate total RNA from cultured HSCs for RNA sequencing

(RNA-seq), as we previously did.[6,23] Details are found in the Supporting Information. Data are found in the Gene Expression Omnibus (GSE127964).

HSC/TUMOR CO-INJECTION MOUSE MODEL

Animal studies were approved by the Institutional Animal Care and Use Committee of University of Minnesota. To assess the effect of HSCs on tumor growth *in vivo*, HT29 cells (0.5×10^6) were mixed with HSCs (0.5×10^6) and co-injected into 8-week-old male nude mice (553; Charles River Laboratories, Wilmington, MA) subcutaneously.[5,6] Tumor sizes were measured with a caliper at different days, and tumor volumes were calculated using the following equation: tumor volume = $(\text{width})^2 \times \text{length}/2$. Tumor growth curves were generated using the GraphPad Prism 5 software (GraphPad Software, Inc., La Jolla, CA).

STATISTICS

All data are expressed as mean ± SD. Statistical analyses were done using two-tailed Student *t* test or analysis of variance (ANOVA) followed by *post hoc* tests (GraphPad Software, Inc., La Jolla, CA). $P < 0.05$ was considered as different.

Results

TARGETING KINASE ACTIVITY OF FAK REDUCED TGFβR2 PROTEIN LEVEL AND MYOFIBROBLASTIC ACTIVATION OF HSCs INDUCED BY TGFβ

FAK is not only a Y kinase but also a protein scaffold, and both functions contribute to signaling. To test whether the kinase activity of FAK influenced the biology of TGFβR2, we used two approaches to disrupt the kinase activity of FAK in HSCs: (1) PF228 (10 μM) was used to inhibit autophosphorylation of FAK at Y397; and (2) a construct encoding FAKY397F mutant, in which Y397 was replaced by F, was generated and expressed in cells. HSCs expressing wild-type FAK (FAKwt) were used as controls. Both approaches were complementary to ensure that results generated by PF228 were not caused by any off-target effect of PF228. HSCs incubated with PF228 were collected for WB for TGFβR2 protein. As revealed by WB, PF228 induced a time-dependent down-regulation of TGFβR2 protein (Fig. 1A, $P < 0.05$). HSCs expressing FAKwt or FAKY397F by retroviral transduction were also collected for WB, which consistently showed that FAKY397F mutant reduced TGFβR2 protein compared with FAKwt (Fig. 1B, $P < 0.05$). Overexpression of FLAG-tagged FAKwt or mutant and suppression of FAK phosphorylation at Y397 by either reagent were confirmed by WB (Fig. 1A,B). Real-time quantitative PCR revealed that TGFβR2 messenger RNA level was not significantly reduced by PF228 or FAKY397F mutant (Supporting Fig. S1A,B). Additionally, HSCs expressing FLAG-tagged TGFβR1 by retroviral transduction[4] were also incubated with PF228 or transduced with FAKY397F retroviruses, and cells were collected for WB for TGFβR1-FLAG. In contrast to TGFβR2, TGFβR1-FLAG protein level was not reduced by PF228 or FAKY397F (Supporting Fig. S1C,D). Thus, the kinase activity of FAK stabilizes TGFβR2 at a post-translational level.

HSCs stimulated with TGFβ1 (5 ng/mL) for 30 minutes or 24 hours were collected for WB to study the role of FAK for TGFβ signaling and HSC activation. As shown in Fig. 1C,D, stimulation of HSCs with TGFβ1 for 30 minutes led to SMAD phosphorylation, and this effect of TGFβ1 was reduced by FAKY397F mutant or PF228 ($P < 0.05$). As assessed by WB for HSC activation markers, α-SMA, fibronectin or CTGF, TGFβ1 stimulation for 24 hours induced up-regulation of α-SMA, fibronectin, or CTGF in control HSCs, and this effect of TGFβ1 was inhibited by FAKY397F mutant or PF228 (Fig. 2A,B, top; $P < 0.05$). α-SMA IF revealed that more than 50% of control HSCs were differentiated into myofibroblasts by TGFβ1, whereas less than 10% of FAKY397F-expressing HSCs and 20% of PF228-incubated HSCs were differentiated under a same condition (Fig. 2A,B, bottom; $P < 0.05$). Moreover, TGFβR2 protein and myofibroblastic activation of HSCs induced by TGFβ1 were suppressed by PF228 in a dose-dependent manner (Supporting Fig. S2A,B; $P < 0.05$). Thus, the kinase activity of FAK regulates TGFβR2 abundance and TGFβ1-stimulated activation of HSCs into myofibroblasts.

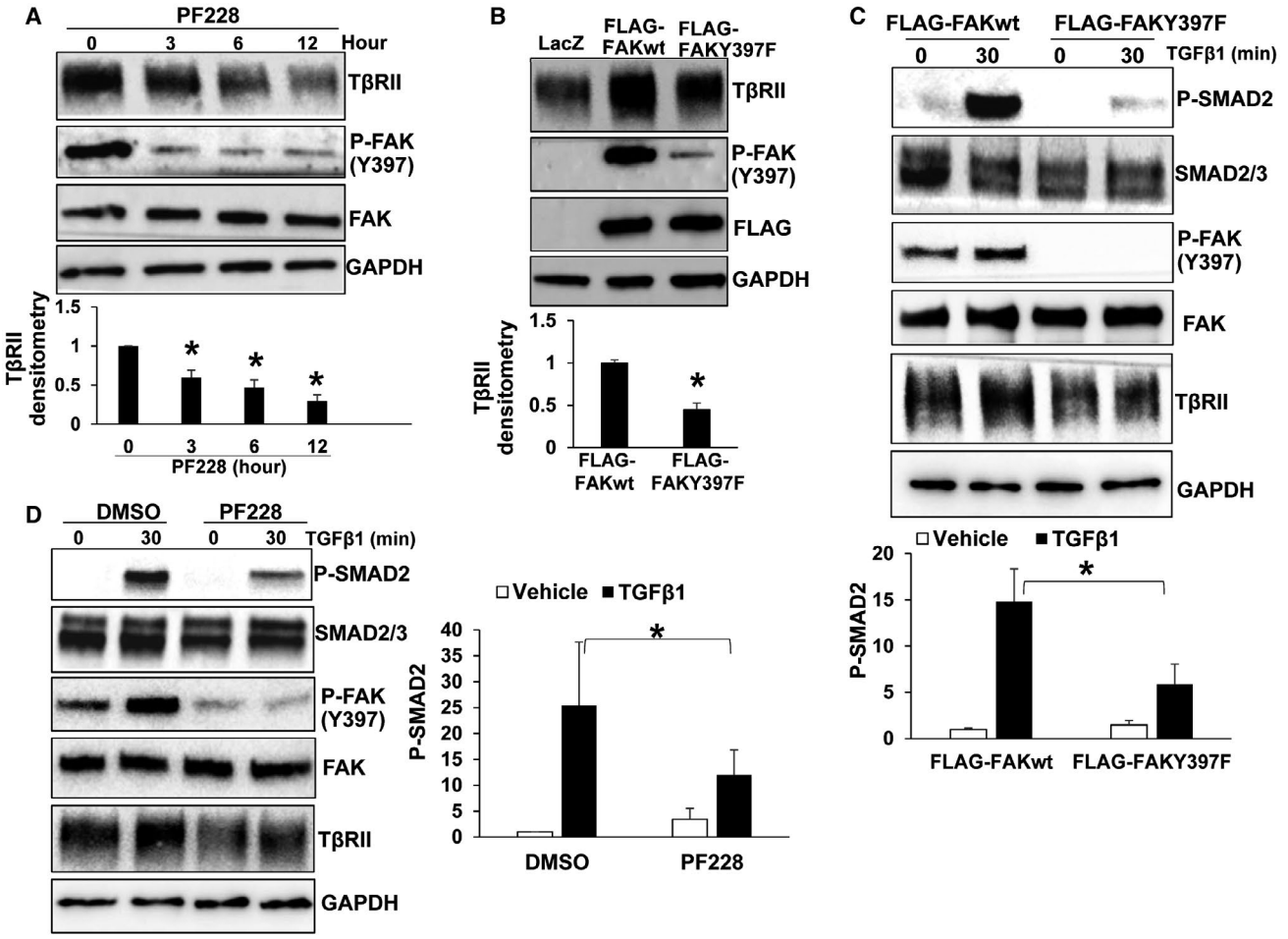

FIG. 1. Inactivation of FAK reduces TGFβR2 protein level and TGFβ1-mediated SMAD phosphorylation. (A) HSCs incubated with PF228 (10 μM) were collected for WB. PF228 down-regulated TGFβR2 in a time-dependent manner. Densitometry was done using the Image J software, and data are shown on the bottom. **P* < 0.05, by ANOVA; n = 3. (B) HSCs expressing FAKwt or FAKY397F mutant were collected for WB. FAKY397F reduced TGFβR2 protein. **P* < 0.05 by *t* test; n = 3. (C) HSCs expressing FAKwt or FAKY397F were stimulated with TGFβ1 (5 ng/mL) and collected for WB. FAKY397F reduced SMAD2 phosphorylation induced by TGFβ1. **P* < 0.05 by ANOVA; n = 3. (D) WB revealed that SMAD2 phosphorylation induced by TGFβ1 was reduced by PF228. **P* < 0.05 by ANOVA; n = 3. Abbreviations: ECM, extracellular matrix; GAPDH, glyceraldehyde 3-phosphate dehydrogenase.

TARGETING THE KINASE ACTIVITY OF FAK PROMOTES UBIQUITINATION AND LYSOSOMAL DEGRADATION OF TGFβR2

To understand how targeting the kinase activity of FAK induced down-regulation of TGFβR2, HSCs incubated with lysosomal inhibitor (bafilomycin [BAF], chloroquine, or E64d + Pepstatin A [PepA]) or proteasomal inhibitor (MG132) were collected for WB. Lysosomal inhibitors, but not proteasomal inhibitor MG132, prevented TGFβR2 down-regulation induced by PF228 or FAKY397F (Fig. 3A,B; $P < 0.05$), suggesting that targeting the kinase activity of FAK led to lysosomal degradation of TGFβR2. This hypothesis was next tested by double IF for TGFβR2 and lysosomal-associated membrane protein 1 (LAMP1), a marker of late endosome/lysosomes.[4] Because commercially available anti-TGFβR2 antibodies were poor for IF, HSCs transduced with retroviruses encoding TGFβR2-HA were incubated with PF228 alone or in combination with BAF, and cells were collected for double

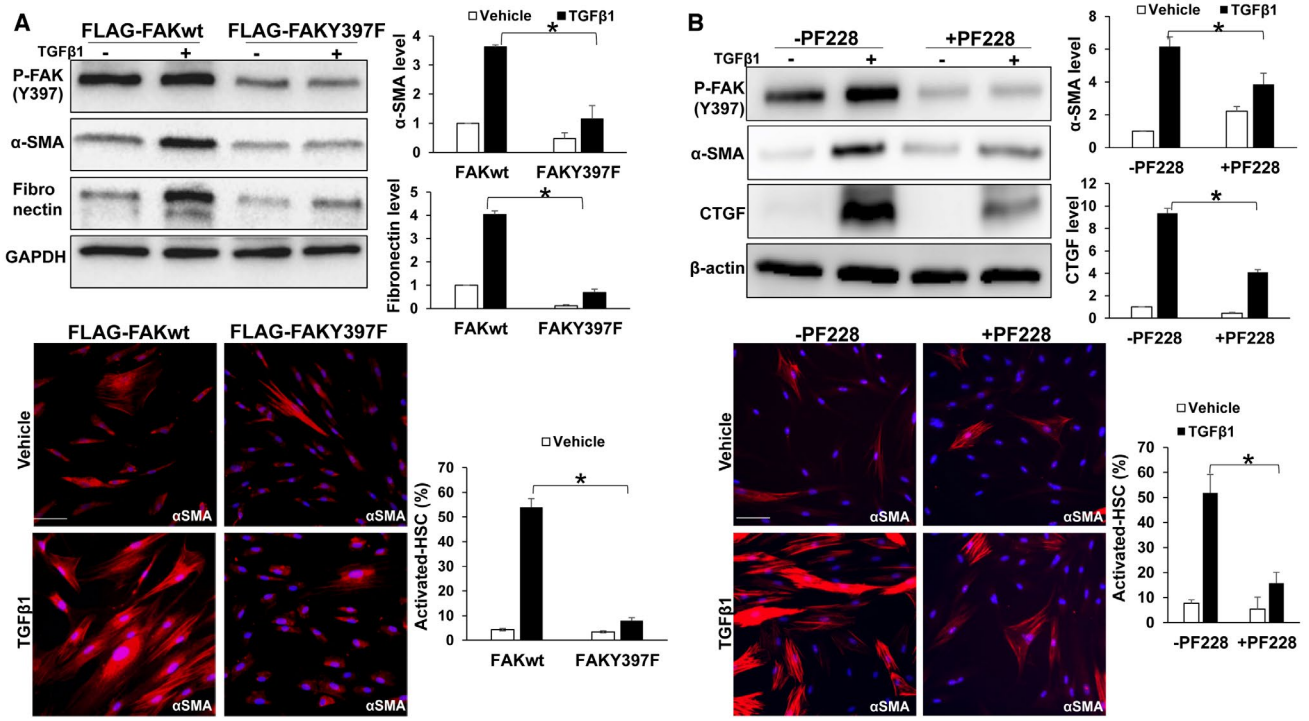

FIG. 2. Inactivation of FAK suppresses myofibroblastic activation of HSCs induced by TGFβ1. (A) Top: HSCs expressing FAKwt or FAKY397F were treated with TGFβ1 for 24 hours and collected for WB. TGFβ1-mediated up-regulation of α-SMA and fibronectin was inhibited by FAKY397F. **P* < 0.05 by ANOVA; n = 3. Bottom: α-SMA IF showed that FAKY397F suppressed TGFβ1-induced myofibroblastic activation of HSCs. **P* < 0.05 by ANOVA; n = 5 randomly picked microscopic fields, each containing 50-100 cells. Bar, 100 μm. (B) Top: WB revealed that TGFβ1-mediated up-regulation of α-SMA and CTGF was inhibited by PF228. **P* < 0.05 by ANOVA; n = 3. Bottom: α-SMA IF showed that PF228 inhibited TGFβ1-induced activation of HSCs into myofibroblasts. **P* < 0.05 by ANOVA; n = 6 randomly picked microscopic fields, each containing 100-200 cells. Bar, 100 μm.

IF for HA and LAMP1. Double IF demonstrated that the percentage of TGFβR2-HA/LAMP1 colocalization in HSCs was increased by PF228 and further enhanced by lysosomal inhibitor BAF (Fig. 3C; *P* < 0.05). Additionally, we tested whether PF228 promoted TGFβR2 ubiquitination, thereby directing TGFβR2 to lysosomes. Because commercial anti-TGFβR2 antibodies were poor for IP, HSCs expressing TGFβR2-HA were used for IP to pull down TGFβR2-HA, followed by WB, to quantitate TGFβR2 ubiquitination. Due to ubiquitination-directed degradation, lower levels of TGFβR2 ubiquitination were detected in dimethyl sulfoxide (DMSO)-incubated and PF228-incubated HSCs, which exhibited a smear pattern (Fig. 3D). Inhibition of lysosomes by BAF blocked degradation of ubiquitinated TGFβR2, and therefore allowed higher levels of TGFβR2 ubiquitination were detected in DMSO/BAF-incubated and PF228/BAF-incubated HSCs (Fig. 3D). The fact that TGFβR2 ubiquitination was higher in PF228/BAF-incubated HSCs than in DMSO/BAF-incubated HSCs indicates that PF228 promoted TGFβR2 ubiquitination. Thus, targeting the kinase activity of FAK led to ubiquitination and lysosomal degradation of TGFβR2.

FAK PROMOTES PLASMA MEMBRANE LOCALIZATION OF TGFβR2

TGFβR2 undergoes constitutive endocytosis in the absence of TGFβ1, followed by lysosomal targeting and degradation.[24,25] The finding that targeting FAK led to lysosomal sorting suggested that FAK may stabilize TGFβR2 protein by keeping it at the plasma membrane. To test this hypothesis, HSCs expressing TGFβR2-HA were transduced by retroviruses encoding either FLAG-FAKwt or FLAG-FAKY397F, and cells were collected

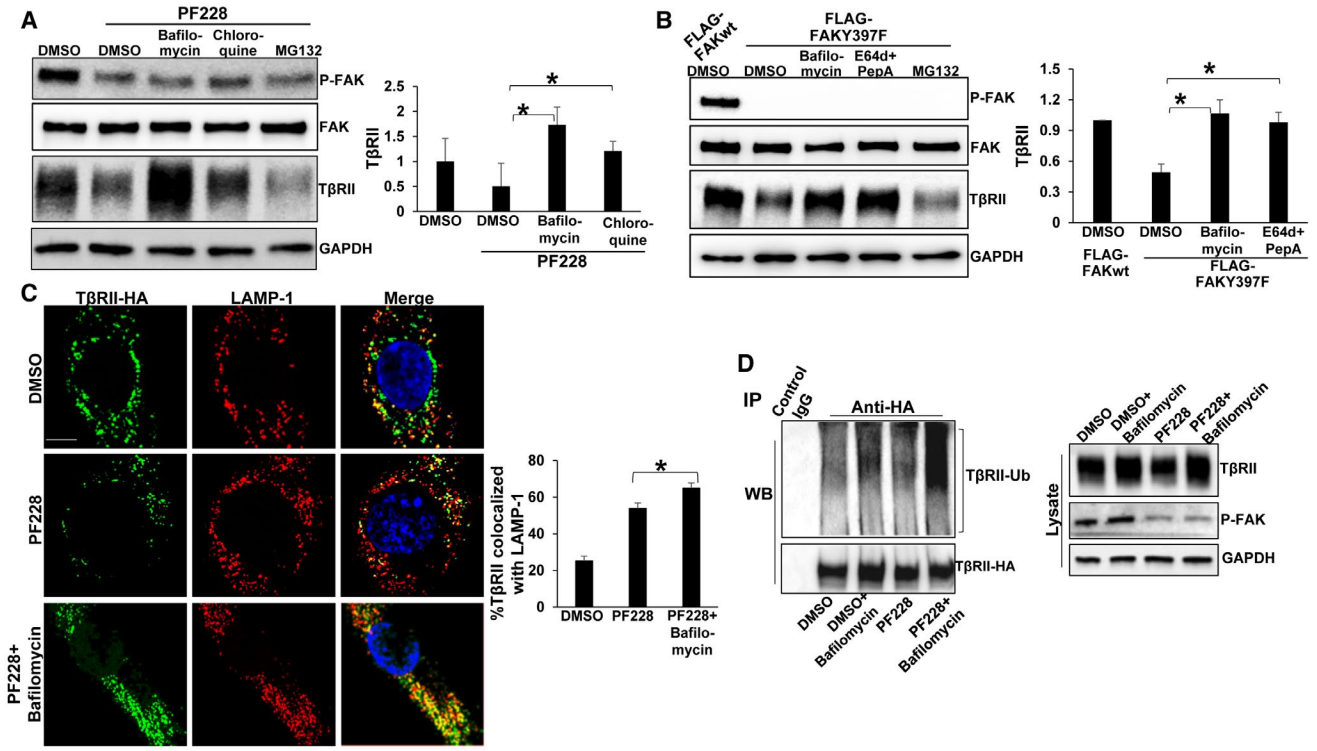

FIG. 3. Targeting FAK promotes ubiquitination and lysosomal degradation of TGFβR2. (A) HSCs incubated with PF228 alone or in combination with a lysosomal inhibitor (BAF 10 nM or chloroquine 50 μM) or proteasomal inhibitor (MG132 25 μM) were collected for WB. A lysosomal inhibitor, but not proteasomal inhibitor, prevented PF228-mediated TGFβR2 down-regulation. **P* < 0.05 by ANOVA; n = 3. (B) HSCs expressing FAKwt or FAKY397F were incubated with DMSO or inhibitors as indicated and cells were collected for WB. E64d (10 μg/mL) + PepA (10 μg/mL) inhibited lysosomes. Lysosomal inhibitors prevented TGFβR2 down-regulation induced by FAKY397F mutant. **P* < 0.05 by ANOVA; n = 3. (C) HSCs expressing TGFβR2-HA were incubated with PF228 alone or in combination with BAF, and cells were collected for IF for HA and LAMP-1. TGFβR2-HA/LAMP-1 colocalization was increased by PF228 and further enhanced by PF228/BAF cotreatment. **P* < 0.05 by ANOVA; n > 6 cells per group. Bar, 10 μm. (D) TGFβR2-HA was precipitated by IP followed by WB using anti-ubiquitin. TGFβR2 ubiquitination was higher in PF228/BAF-incubated HSCs than in BAF-incubated HSCs. Data are representative of multiple repeats with consistent results.

for double IF for FLAG and HA. Colocalization of FAK and TGFβR2-HA at the plasma membrane was detected in FLAG-FAKwt-expressing HSCs (Fig. 4A, arrows), but not in FLAG-FAKY397F-expressing cells (Fig. 4A, bottom panels). Biotinylation of cell surface proteins followed by streptavidin-agarose pulldown confirmed that overexpression of FLAG-FAKwt promoted plasma membrane TGFβR2-HA but overexpression of FLAG-FAKY397F did not (Fig. 4B; $P < 0.05$). Consistently, plasma membrane colocalization of FAK/TGFβR2-HA was reduced by PF228 (Supporting Fig. S3A,B; $P < 0.05$). Moreover, interactions between endogenous FAK and TGFβR2 in HSCs were confirmed by Duolink proximity ligation assay (Supporting Fig. S3C). Thus, FAK kinase activity is required for localization of TGFβR2 at the plasma membrane.

Phosphorylation of FAK was detected in both control HSCs and FLAG-FAKwt-expressing HSCs by WB (Fig. 2A,B), suggesting that a fraction of FAK in HSCs was activated, possibly by the stiff culture substrate and/or growth factors in the culture medium.[12,26] Therefore, we investigated whether streptavidin agarose could pull down both biotinylated TGFβR2 and activated FAK. Indeed, phosphorylated FAK (p-FAK) Y397 was coprecipitated with biotinylated TGFβR2-HA (Fig. 4B), suggesting that active FAK formed a complex with TGFβR2-HA at the plasma membrane. This was further supported by double IF for p-FAKY397 and TGFβR2-HA (Fig. 4C, arrows). Coimmunoprecipitation (coIP) demonstrated that TGFβR2/FAKwt binding was strong, whereas TGFβR2/FAKY397F binding was very weak in HSCs

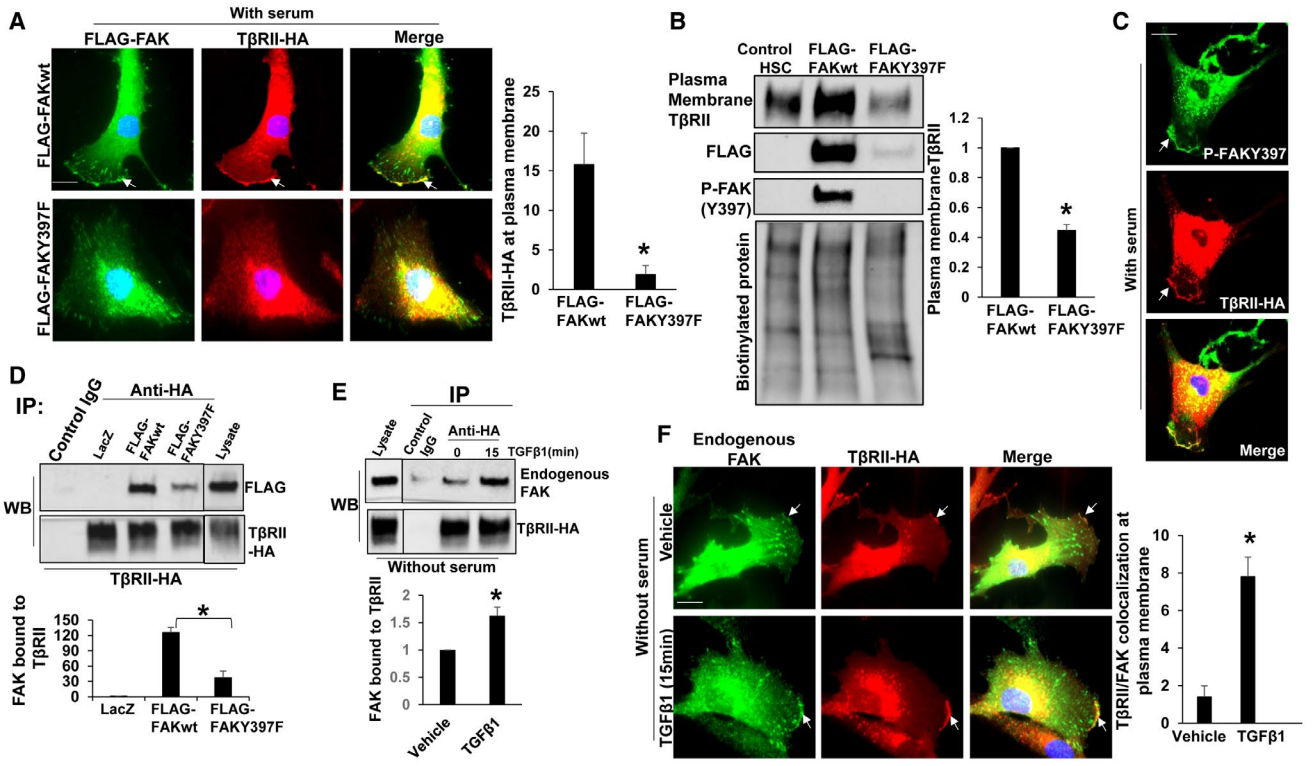

FIG. 4. FAK promotes plasma membrane localization of TGFβR2. (A) HSCs expressing TGFβR2-HA and FLAG-tagged FAK were collected for double IF. FAK/TGFβR2 colocalization at the plasma membrane was detected in HSCs expressing FAKwt but not in HSCs expressing FAKY397F. IF data were quantitated by the ImageJ software and data are shown on the right. **P* < 0.05 by *t* test; n > 8 cells per group. Bar, 20 μm. (B) Biotinylation of cell surface proteins followed by streptavidin agarose pulldown revealed that FAKwt, but not FAKY397F, increased plasma membrane TGFβR2. **P* < 0.05 by *t* test; n = 3. (C) Double IF showed that TGFβR2-HA colocalized with phosphorylated FAK at the plasma membrane (arrows). Bar, 20 μm. (D) CoIP revealed that FAK/TGFβR2 binding in HSCs was abolished by Y397 to F mutation on FAK. **P* < 0.05 by ANOVA; n = 3. (E) CoIP revealed that stimulation of HSCs with TGFβ1 for 15 minutes promoted FAK/TβRII-HA binding. **P* < 0.05 by *t* test; n = 3. (F) Double IF demonstrated that TGFβ1 stimulation promoted FAK/TGFβR2 colocalization at the plasma membrane. **P* < 0.05 by *t* test; n > 8 cells per group. Bar, 20 μm. Abbreviation: IgG, immunoglobulin.

(Fig. 4D; *P* < 0.05). Thus, TGFβR2 and active FAK interacted at the plasma membrane of HSCs.

TGFβ1 PROMOTES PLASMA MEMBRANE TARGETING OF TGFβR2 BY ACTIVATING FAK

Because TGFβ1 induces FAK phosphorylation and activation in various cell types,[14,18,27] we performed WB and confirmed the finding that stimulation of HSCs with TGFβ1 for 15 or 30 minutes increased FAK phosphorylation at Y397 (Supporting Fig. S4; *P* < 0.05). We next tested whether TGFβ1 regulated plasma membrane targeting of TGFβR2 by activating FAK. CoIP revealed that TGFβ1 stimulation indeed increased TGFβR2-HA/FAK binding in HSCs (Fig. 4E; *P* < 0.05), and double IF showed that in serum-starved HSCs, the level of colocalization of TGFβR2-HA with endogenous FAK at the plasma membrane was low and it was increased following TGFβ1 stimulation (Fig. 4F; *P* < 0.05). Additionally, stimulation of HSCs with TGFβ1 for 30 minutes increased the TGFβR2 protein level, and this effect of TGFβ1 was attenuated by expression of FAKY397F mutant or PF228 (Fig. 1C,D). Thus, short-term stimulation of HSCs by TGFβ1 led to FAK activation and colocalization of FAK/TGFβR2 at the plasma membrane of HSCs.

Y336 OF TGFβR2 IS PHOSPHORYLATED BY FAK

Because active FAK bound to TGFβR2, we investigated whether TGFβR2 was a phosphorylation substrate of FAK. HSCs expressing TGFβR2-HA were collected for IP using anti-phosphorylated tyrosine (PY) (4G10) to pull down Y-phosphorylated proteins, and WB was followed to quantitate TGFβR2-HA within the precipitates, which represented Y-phosphorylated TGFβR2-HA. As shown in Fig. 5A, TGFβR2-HA was readily detected from the precipitates of control HSCs but barely detected from those of PF228-incubated cells ($P < 0.05$ by t test), suggesting that TGFβR2-HA was phosphorylated by FAK. Because TGFβ1 promoted FAK/TβRII binding (Fig. 4E,F), we collected HSCs stimulated with TGFβ1 for IP using anti-PY (4G10) followed by WB. As expected, stimulation of HSCs with TGFβ1, for either 5 or 15 minutes, increased Y phosphorylation of TGFβR2 (Fig. 5B; $P < 0.05$), suggesting that short-term TGFβ1 stimulation promotes FAK/TGFβR2 binding and TGFβR2 Y phosphorylation.

It has been reported that Y259, Y336, and Y424 were autophosphorylated by TGFβR2,[28] so we generated three HA-tagged mutants, TβRIIY259F-HA, TβRIIY336F-HA and TβRIIY424F-HA, to investigate whether any Y was phosphorylated by FAK in

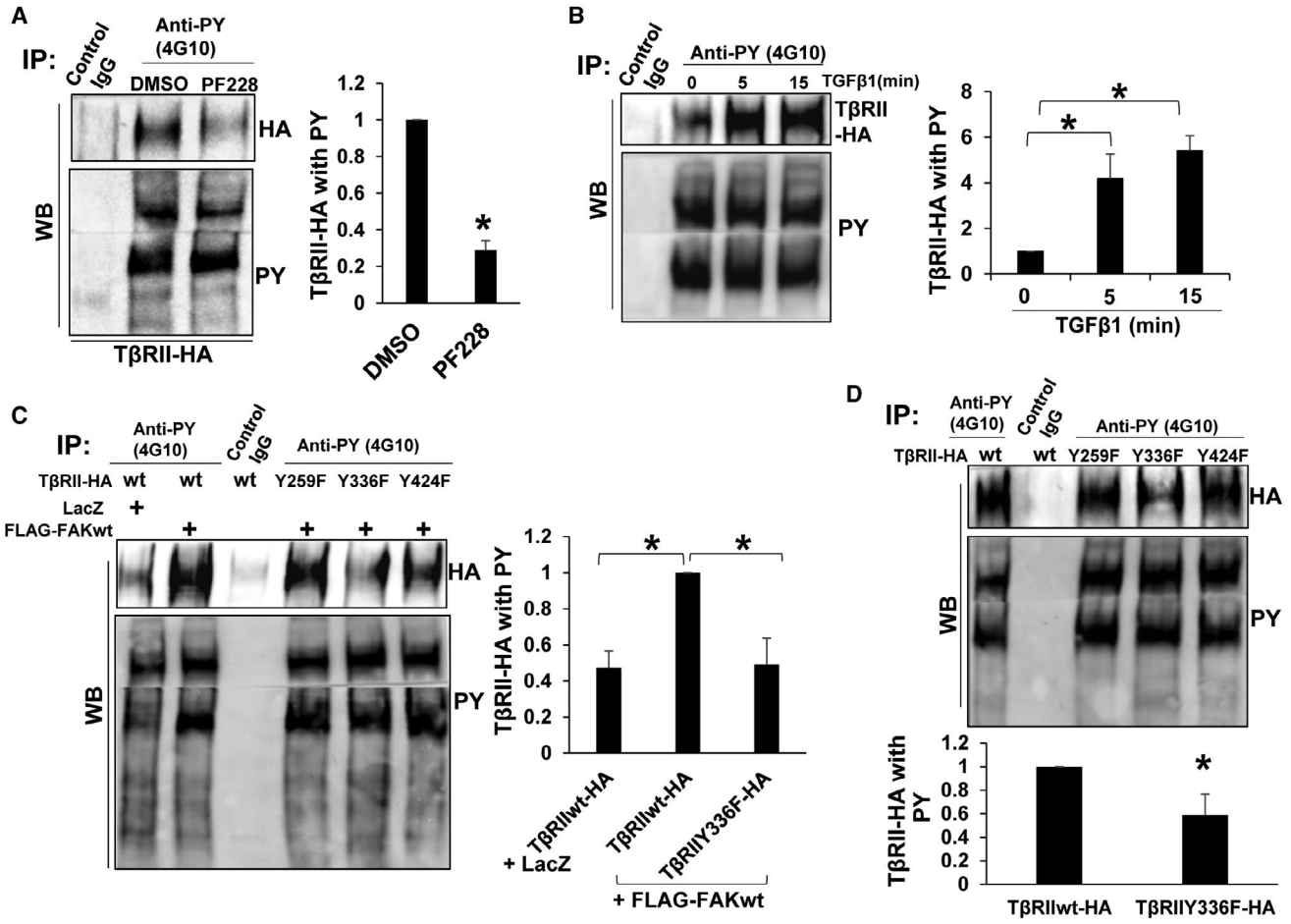

FIG. 5. Y336 of TGFβR2 is phosphorylated by FAK. (A) HSCs expressing TGFβR2-HA were collected for IP using anti-PY (4G10) followed by WB for TGFβR2. PF228 reduced the level of Y phosphorylation of TGFβR2. *$P < 0.05$ by t test; n = 3. (B) TGFβ1 stimulation increased Y phosphorylation of TGFβR2. *$P < 0.05$ by ANOVA; n = 3. (C) HSCs expressing HA-tagged wild-type TGFβR2 or mutant were transduced with LacZ or FAKwt retroviruses, and cells were collected for IP followed by WB to quantitate Y phosphorylation of TGFβR2. FAKwt increased Y phosphorylation of TGFβR2, and this effect of FAK was abrogated by mutating Y336 to F on TGFβR2. *$P < 0.05$ by ANOVA; n = 3. (D) Mutating Y336 to F on TGFβR2 reduced Y phosphorylation of TGFβR2 induced by endogenous FAK. *$P < 0.05$ by t test; n = 3. Abbreviation: IgG, immunoglobulin.

HSCs. HSCs expressing TGFβR2wt-HA or a mutant were transduced again with LacZ or FLAG-FAKwt retroviruses, and cells were collected for IP using anti-PY (4G10). As shown in Fig. 5C, overexpression of FAKwt increased Y phosphorylation of TGFβR2 compared with overexpression of LacZ, and this increase was abrogated by Y336F mutation on TGFβR2 ($P < 0.05$), but not by Y259F or Y424F mutation. Additionally, HSCs expressing endogenous FAK were collected for IP, which confirmed that Y336F mutation on TGFβR2 reduced Y phosphorylation of TGFβR2 induced by endogenous FAK (Fig. 5D, $P < 0.05$). Thus, Y336 of TGFβR2 was phosphorylated by FAK.

MUTATING Y336 TO F LEADS TO LYSOSOMAL DEGRADATION OF TGFβR2

To analyze whether Y336F TGFβR2 mutant recapitulated the phenotypes of TGFβR2 in PF228-incubated or FAKY397F-expressing HSCs, we compared the protein levels of three HA-tagged TGFβR2 mutants by WB. The TGFβR2Y336F-HA protein level was the lowest among all groups, indicating that the protein stability of TGFβR2 was reduced by Y336 to F mutation (Fig. 6A; $P < 0.05$). Next, HSCs incubated with cycloheximide for different times (cycloheximide-blocked protein synthesis) were collected for WB to analyze the protein stability of TGFβR2wt-HA and TGFβR2Y336F-HA. The half-life was 106.5 minutes for TGFβR2wt-HA and 70.6 minutes for TGFβR2Y336F-HA, suggesting that TGFβR2Y336F-HA degraded much faster than TGFβR2wt-HA (Fig. 6B; $P < 0.05$ by ANOVA). To study how TGFβR2Y336F-HA degraded, HSCs incubated with either lysosomal inhibitor (BAF, E64d + Pepstatin A) or proteasomeal inhibitor (MG132) were collected for WB. Although both lysosomal and proteasomal inhibitors prevented the degradation of TGFβR2wt-HA, only lysosomal inhibitors prevented the degradation of TGFβR2Y336F-HA in HSCs (Fig. 6C; $P < 0.05$), supporting that TGFβR2Y336F-HA was downgraded by lysosomes.

TGFβR2Y336F-HA MUTANT SUPPRESSES HSC ACTIVATION INDUCED BY TGFβ

Although TGFβR2Y336F-HA was not as stable as TGFβR2wt-HA, we still introduced it into HSCs to test whether its overexpression influenced TGFβ1 signaling of HSCs. HSCs expressing LacZ (control) or TGFβR2Y336F-HA by retroviral transduction were stimulated with TGFβ1 and collected for WB. Overexpression of TGFβR2Y336F-HA mutant was confirmed by WB for HA (Fig. 6D). In LacZ-expressing cells, TGFβ1 up-regulated HSC activation markers, fibronectin, α-SMA, and CTGF, and this effect of TGFβ1 was suppressed by TGFβR2Y336F-HA mutant (Fig. 6D; $P < 0.05$). Thus, TGFβR2Y336F functioned as a dominant negative mutant to suppress HSC activation.

FAK INACTIVATION SUPPRESSES TUMOR-PROMOTING EFFECTS OF HSCs *IN VITRO* AND IN MICE

We have shown previously that activated HSC/myofibroblasts promoted tumor cell growth,[4-6] so we used *in vitro* and *in vivo* studies to analyze the role of FAK for the paracrine tumor-promoting effect of HSCs. Because the liver is an organ frequently colonized by metastatic colorectal cancer cells, we tested whether HSC FAK influenced the interactions between HSCs and metastatic colorectal cancer cells. To this end, HT29 human colorectal cancer cells were chosen for the studies. Conditioned medium (CM) was collected from HSCs, and its role for HT29 proliferation was analyzed by MTS (3-[4,5-dimethylthiazol-2-yl]-5-[3-carboxymethoxyphenyl]-2-[4-sulfophenyl]-2*H*-tetrazolium) assay. As shown in Fig. 7A (top), the CM of HSCs expressing FLAG-FAKwt promoted HT29 proliferation compared with the basal culture medium ($P < 0.05$). Importantly, the CM of FLAG-FAKY397F expressing HSCs was less effective at promoting HT29 proliferation than the CM of HSCs expressing FLAG-FAKwt ($P < 0.05$ by ANOVA). Consistently, the CM of FAK knockdown HSCs was less effective than that of control HSCs (Fig. 7A, bottom; $P < 0.05$ by ANOVA). Thus, inactivation of FAK reduced the tumor-promoting effect of HSCs *in vitro*.

Next, HT29 (0.5×10^6 cells) were mixed with HSCs (0.5×10^6 cells) *in vitro*, and they were co-injected into nude mice subcutaneously. Tumor growth was measured by a caliper at different days after co-implantation, and data are shown in Fig. 7B. Consistent with MTS assay, HSCs expressing FLAG-FAKY397F were less effective at promoting HT29 growth in mice

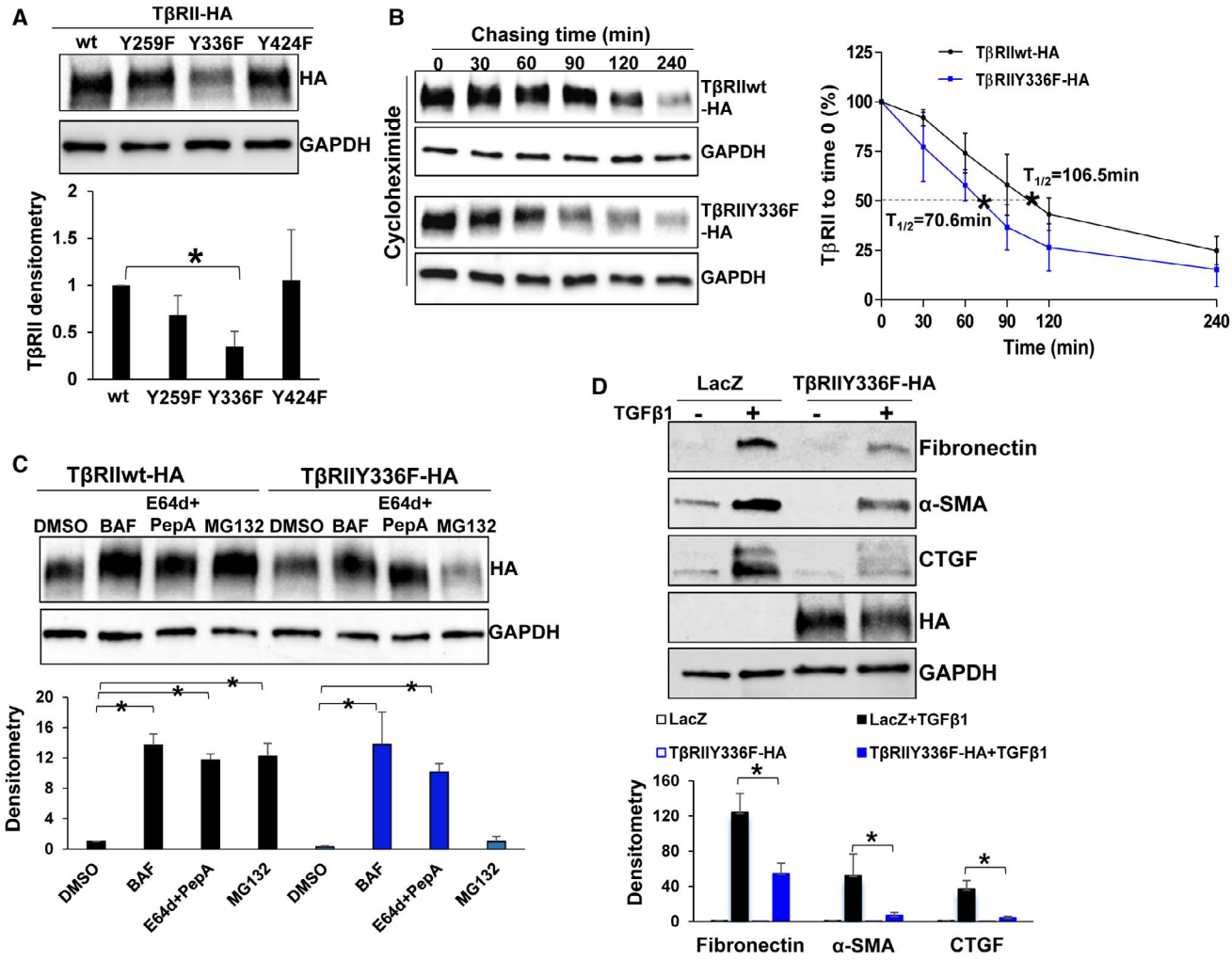

FIG. 6. Mutating Y336 to F on TGFβR2 leads to lysosomal degradation of TGFβR2. (A) WB revealed that the protein level of TGFβR2Y336F mutant was lowest among all groups. **P* < 0.05 by *t* test; n = 3. (B) HSCs incubated with cycloheximide for different times were collected for WB. Y336 to F mutation on TGFβR2 reduced its half-life. **P* < 0.05 by ANOVA; n = 3. (C) HSCs incubated with lysosomal inhibitors, BAF, E64d + Pepstatin A, or proteasomal inhibitor MG132 were collected for WB. TGFβR2wt degradation was prevented by either lysosomal or proteasomal inhibitor, whereas TGFβR2Y336F degradation was prevented by lysosomal inhibitor only. **P* < 0.05 by ANOVA; n = 3. (D) HSCs expressing LacZ or TGFβR2Y336F mutant by retroviral transduction were stimulated by TGFβ1 and collected for WB. Overexpression of TGFβR2Y336F mutant suppressed HSC activation induced by TGFβ1. **P* < 0.05 by ANOVA; n = 3.

than HSCs expressing FLAG-FAKwt (Fig. 7B, top and middle; $P < 0.05$), and FAK knockdown HSCs were less effective than control HSCs (Fig. 7B, bottom; $P < 0.05$). WB and IF revealed that myofibroblast densities were reduced in tumors arising from HT29/HSC-FAKY397F or HT29/HSC-FAKshRNA co-injections, compared with tumors arising from control co-injections (Fig. 7C,D; $P < 0.05$ by ANOVA). Thus, FAK is required for activation of HSCs into tumor-promoting myofibroblasts *in vivo*.

TARGETING FAK BLOCKS HSCs TO PRODUCE TUMOR-PROMOTING FACTORS

Microarray analysis helped us identify HSC-derived tumor-promoting factors, including tenascin C, periostin, and CTGF in response to TGFβ1 stimulation.[6] To search for FAK-dependent tumor-promoting factors of HSCs, we collected HSCs incubated with PF228 and TGFβ1 for RNA-seq.

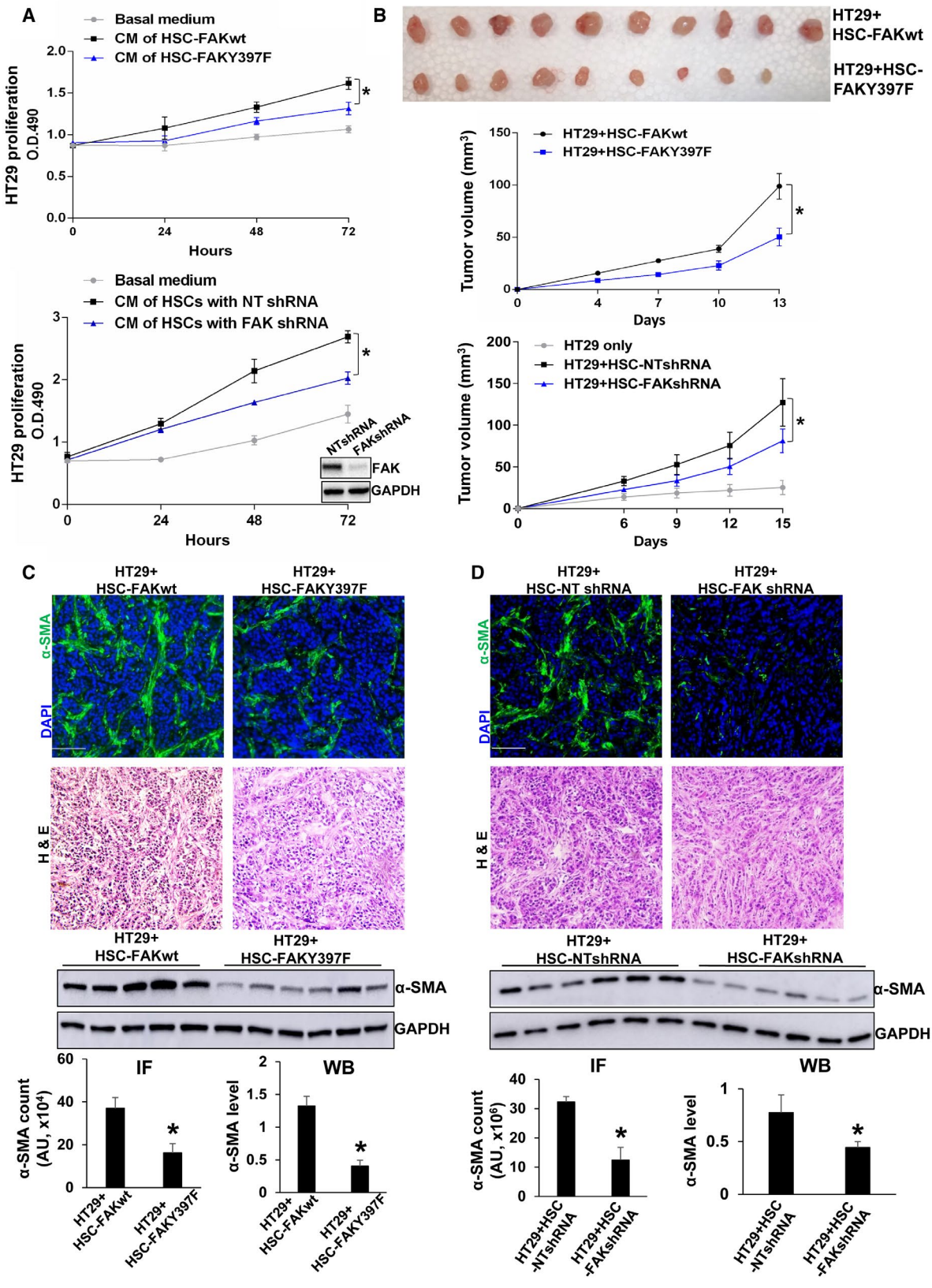
A
Basal medium
CM of HSC-FAKwt
CM of HSC-FAKY397F
HT29 proliferation O.D.490
Hours
Basal medium
CM of HSCs with NT shRNA
CM of HSCs with FAK shRNA
NTshRNA
FAKshRNA
FAK
GAPDH
B
HT29+ HSC-FAKwt
HT29+HSC-FAKY397F
HT29+HSC-FAKwt
HT29+HSC-FAKY397F
Tumor volume (mm3)
Days
HT29 only
HT29+HSC-NTshRNA
HT29+HSC-FAKshRNA
C
HT29+ HSC-FAKwt
HT29+ HSC-FAKY397F
α-SMA
DAPI
H & E
α-SMA
GAPDH
IF
WB
α-SMA count (AU, x10⁴)
α-SMA level
D
HT29+ HSC-NT shRNA
HT29+ HSC-FAK shRNA
HT29+ HSC-NTshRNA
HT29+ HSC-FAKshRNA
α-SMA count (AU, x10⁶)

FIG. 7. FAK inactivation suppresses tumor-promoting effects of HSCs *in vitro* and in tumor implantation mouse model. (A) MTS assays showed that the CM of FAKY397F-expressing or FAK-knockdown HSCs was less effective at promoting HT29 proliferation than that of control HSCs. **P* < 0.05 by ANOVA; n = 5. (B) HT29 (0.5×10^6) were mixed with HSCs (0.5×10^6), and cells were coinjected into nude mice subcutaneously. FAKY397F-expressing or FAK-knockdown HSCs were less effective at promoting HT29 growth in mice than control HSCs. **P* < 0.05 by ANOVA, n = 10, 6. (C) WB and IF revealed that myofibroblast densities were lower in tumors arising from HT29/HSC-FAKY397F co-injections than in tumors arising from control coinjections. **P* < 0.05 by *t* test; n = 3 tumors for IF and n = 5, 6 for WB. Bar, 50 μm. (D) Myofibroblast densities were lower in tumors arising from HT29/HSC-FAKshRNA co-injections than in tumors arising from control co-injections. **P* < 0.05 by *t* test; n = 3 tumors for IF and n = 6 for WB. Bar, 50 μm. Abbreviations: DAPI, 4′,6-diamidino-2-phenylindole; H&E, hematoxylin and eosin staining; NT shRNA, nontargeting short hairpin RNA.

As shown in Supporting Fig. S5, the transcripts of 764 genes were affected by PF228 in TGFβ1-stimulated HSCs. Of the 764 genes, 20 genes that encode tumor-promoting factors were turned on by TGFβ1 for transcription in a FAK-dependent manner (Fig. 8A). Most of these genes could be divided into two groups: genes encoding extracellular matrix remodeling proteins, such as COL5A1, COL7A1, COL16A1, TNC, SPARC, EDIL3, ADAMTS1, MMP3, and MMP10, and genes encoding growth factors and cytokines, such as NGF, FGF1, FGF2, LIF, TGFβ1, TGFβ2, VEGFA, CTGF, and interleukin 11 (Fig. 8A). Interestingly, the CD274 gene, encoding immune checkpoint molecule PD-L1, was also a FAK-dependent TGFβ1 target. PD-L1 was relevant to patients with colorectal cancer, although

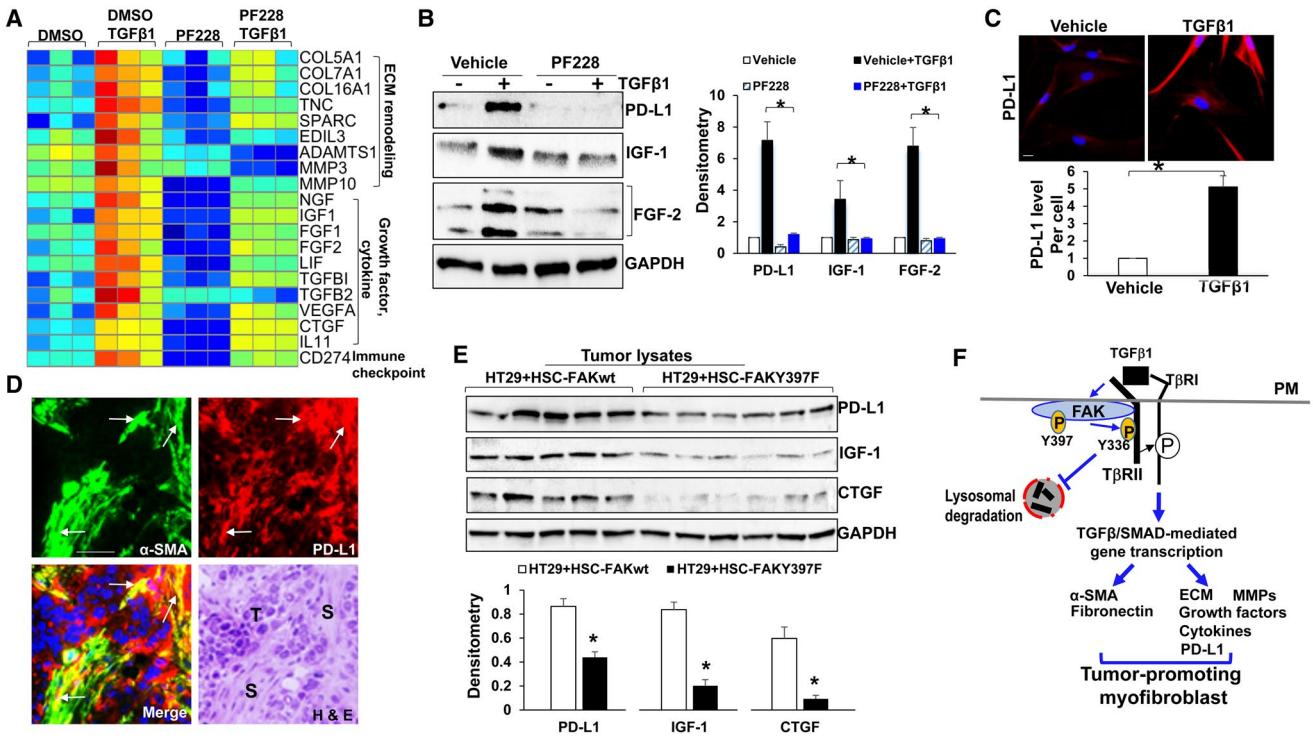

FIG. 8. FAK inactivation suppresses HSC-derived tumor-promoting paracrine factors. (A) RNA-seq identified 20 representative genes, encoding tumor-promoting factors, as FAK-dependent TGFβ targets. (B) WB confirmed that TGFβ1 stimulated HSC to produce PD-L1, IGF-1, and FGF2, through FAK. **P* < 0.05 by ANOVA; n = 3. (C) HSCs stimulated with TGFβ1 were collected for IF for PD-L1. and cell nuclei were counterstained by DAPI. **P* < 0.05 by *t* test; n = 25 cells per group. Bar, 20 μm. (D) HT29 tumors, as described in Fig. 7B, were subjected to double IF. Overlap of PD-L1 and α-SMA were detected (arrows). Bar, 50 μm. (E) Tumor lysates, as described in Fig. 7C, were subjected to WB for PD-L1, IGF-1, and CTGF. **P* < 0.05 by *t* test; n = 5,6. (F) A schematic diagram of this study. FAK, after phosphorylation and activation, binds to TGFβR2 and phosphorylates TGFβR2 at Y336, and subsequently targets TGFβR2 to the plasma membrane. Promoted by FAK, TGFβ/SMAD signaling turns on gene transcription to define the phenotypes of activated-HSC/myofibroblasts and produce tumor-promoting factors. Abbreviations: ECM, extracellular matrix; H&E, hematoxylin and eosin staining; P, phosphate group; PM, plasma membrane; S, stroma; T, tumor.

it was not important for this tumor implantation model because the mice used were athymic. WB and IF confirmed that PD-L1 was up-regulated by TGFβ1 through FAK (Fig. 8B,C; $P < 0.05$). Double IF performed with HT29 tumor nodules or murine colorectal liver metastases demonstrated that the activated-HSC/myofibroblasts were indeed a source of PD-L1 (Fig. 8D; Supporting Fig. S6, arrows). Additionally, WB confirmed that TGFβ1 stimulated HSC to produce PD-L1, IGF-1 and FGF-2 through FAK (Fig. 8B; $P < 0.05$) and that the protein levels of PD-L1, IGF-1, and CTGF were reduced in tumors arising from HT29/HSC-FAKY397F co-injections, compared with tumors arising from control injections (Fig. 8E; $P < 0.05$). Furthermore, IF for Ki67 (marker of proliferating cells) and cleaved caspase 3 (marker of apoptotic cells) revealed that the tumor proliferation rate was higher in tumors arising from HT29/HSC-FAKwt co-injections than in tumors arising from HT29/HSC-FAKY397F co-injections, and that reversely, apoptosis rate was lower in tumors arising from HT29/HSC-FAKwt co-injections than in tumors arising from HT29/HSC-FAKY397F co-injections (Supporting Fig. S7; $P < 0.05$). Thus, targeting FAK of HSCs suppressed tumor-promoting paracrine factors and limited tumor growth in mice.

Discussion

Through kinase-dependent and kinase-independent mechanisms, FAK accepts extracellular signals from the plasma membrane receptors and transmit them into the interior of the cell. However, little is known whether FAK in return regulates the biology of the plasma membrane receptors. Our study, using TGFβR2 as a model, demonstrated that FAK was indeed required for subcellular localization of the receptor and its biological function. Mechanistically, active FAK bound to TGFβR2 to induce its phosphorylation at Y336 and targeted it to the plasma membrane of HSCs. In contrast, inactivation of FAK or mutating Y336 to F on TGFβR2 led to a rapid degradation of TGFβR2 by lysosomes (Fig. 8F). Functionally, targeting FAK or Y phosphorylation of TGFβR2 abrogated TGFβ-mediated HSC activation and suppressed HSC-derived tumor-promoting paracrine factors. Thus, FAK represents a target for suppressing HSC activation and the metastasis-promoting liver microenvironment.

In addition to canonical TGF/SMAD signaling, TGFβ activates PI3K/Akt, ERK, p38 MAPK, which are noncanonical TGFβ signaling pathways. These noncanonical TGFβ signaling pathways are known to be regulated by FAK.[14,18,29,30] In addition, FAK contains a nuclear localization signal in its FERM domain through which FAK may enter the nucleus to modulate gene transcription.[8] Thus, FAK may regulate HSC activation through diverse and complicated mechanisms. Nevertheless, our study unveiled an unrecognized mechanism and added knowledge into the field by demonstrating that FAK phosphorylated TGFβR2 at Y336 and targeted it to the plasma membrane. Interestingly, TGFβ1 used this mechanism to call the cytoplasmic TGFβR2 onto the plasma membrane. Because TGFβR2 at the plasma membrane undergoes constitutive endocytosis, this mechanism allows the plasma membrane TGFβR2 be maintained at a consistent level to ensure sustained TGFβ signal transduction.

Previous studies suggested that in breast cancer cells, binding β3 integrin to TGFβR2 led to Y phosphorylation of TGFβR2 at Y284 by Src, which was linked to TGFβ-mediated MAPK activation.[31] To test whether PF228 inhibited Src kinase, we performed WB for P-Src (Y416) and found that PF228 reduced FAK phosphorylation at Y397, whereas it increased Src phosphorylation at Y416 (Supporting Fig. S3D; $P < 0.05$ by t test). Thus, PF228 impaired TGFβR2 Y phosphorylation by targeting FAK, but not Src. How did FAK take TGFβR2 to the plasma membrane of HSCs? It has been reported that hyperphosphorylation of FAK disassociated it from focal adhesions[32] and that phosphorylation of Y925 on FAK and Grb2 SH2 domain binding to this site led to dislocalization of FAK from focal adhesions to the plasma membrane.[33] These findings support a model in which FAK, after its phosphorylation, including phosphorylation at Y925, binds to TGFβR2 and takes it along to the plasma membrane.

We have identified 20 FAK-dependent HSC-derived tumor-promoting paracrine factors by RNA-seq (Fig. 8A). IGF-1 attracted our attention, as both IGF-1 and IGF-2 activate IGFR1. It has been reported that IGFR1-mediated expression of Nanog promotes the formation of cancer stem cells of HCC[34] and the

proliferation of acute myeloid leukemia stem cells,[35] linking to cancer invasion, metastasis, and drug resistance. Tenascin C encoded by TNC regulates cancer stemness by activate Notch signaling of cancer cells.[36] TGFβ1 and TGFβ2 genes were identified, suggesting that HSC activation was in fact a vicious cycle enhanced by a self-made positive feedback loop. Interestingly, CD274, encoding an immune checkpoint protein PD-L1, was identified. A preclinical study showed that FAK inhibitor VS-4718 reduced fibrosis of pancreatic cancer and increased tumor infiltration of cytotoxic T cells, and that additionally, adding VS-4718 to gemcitabine + anti-PD1/anti-CTLA4 combinatorial therapy improved survival of mice.[37] Although PD-L1 is produced by various cell types of a tumor, our data revealed that specific targeting FAK of myofibroblasts reduced the total protein level of PD-L1 of a tumor (Fig. 8E), suggesting that the activated-HSC/myofibroblasts were a significant contributor to PD-L1 of the tumor microenvironment. Thus, in addition to lower tumor-promoting growth factors, cytokines, and extracellular matrix remodeling proteins, targeting FAK of HSC/myofibroblasts may suppress PD-L1/PD1 immune checkpoint and increase tumor infiltration of T cells, so as to improve the efficacy of immunotherapy and combinatorial therapy for patients with metastatic liver disease.

Acknowledgments: We thank Ms. Elyse Froehling, Mr. Aaron Becker, and Juan Abrahante, Ph.D., at the University of Minnesota Genomic Center, for performing the RNA-seq and bioinformatics analysis.

REFERENCES

1) Kang N, Gores GJ, Shah VH. Hepatic stellate cells: partners in crime for liver metastases? Hepatology 2011;54:707-713.
2) Kang N, Shah VH, Urrutia R. Membrane-to-nucleus signals and epigenetic mechanisms for myofibroblastic activation and desmoplastic stroma: potential therapeutic targets for liver metastasis? Mol Cancer Res 2015;13:604-612.
3) Shi Y, Massague J. Mechanisms of TGF-beta signaling from cell membrane to the nucleus. Cell 2003;113:685-700.
4) Liu C, Billadeau DD, Abdelhakim H, Leof E, Kaibuchi K, Bernabeu C, et al. IQGAP1 suppresses TbetaRII-mediated myofibroblastic activation and metastatic growth in liver. J Clin Invest 2013;123:1138-1156.
5) Tu K, Li J, Verma VK, Liu C, Billadeau DD, Lamprecht G, et al. VASP promotes TGF-β activation of hepatic stellate cells by regulating Rab11 dependent plasma membrane targeting of TGF-β receptors. Hepatology (Baltimore, MD) 2015;61:361.
6) Wang Y, Tu K, Liu D, Guo L, Chen Y, Li Q, et al. p300 Acetyltransferase is a cytoplasm-to-nucleus shuttle for SMAD2/3 and TAZ nuclear transport in transforming growth factor beta-stimulated hepatic stellate cells. Hepatology 2019; 70:1409-1423.
7) Sulzmaier FJ, Jean C, Schlaepfer DD. FAK in cancer: mechanistic findings and clinical applications. Nat Rev Cancer 2014; 14:598-610.
8) Kleinschmidt EG, Schlaepfer DD. Focal adhesion kinase signaling in unexpected places. Curr Opin Cell Biol 2017;45:24-30.
9) Frame MC, Patel H, Serrels B, Lietha D, Eck MJ. The FERM domain: organizing the structure and function of FAK. Nat Rev Mol Cell Biol 2010;11:802-814.
10) Plotnikov SV, Pasapera AM, Sabass B, Waterman CM. Force fluctuations within focal adhesions mediate ECM-rigidity sensing to guide directed cell migration. Cell 2012;151:1513-1527.
11) **Chen XL**, **Nam JO**, Jean C, Lawson C, Walsh CT, Goka E, et al. VEGF-induced vascular permeability is mediated by FAK. Dev Cell 2012;22:146-157.
12) Santos AR, Corredor RG, Obeso BA, Trakhtenberg EF, Wang Y, Ponmattam J, et al. Beta1 integrin-focal adhesion kinase (FAK) signaling modulates retinal ganglion cell (RGC) survival. PLoS ONE 2012;7:e48332.
13) Reif S, Lang A, Lindquist JN, Yata Y, Gabele E, Scanga A, et al. The role of focal adhesion kinase-phosphatidylinositol 3-kinase-akt signaling in hepatic stellate cell proliferation and type I collagen expression. J Biol Chem 2003;278:8083-8090.
14) **Liu S**, **Xu SW**, Kennedy L, Pala D, Chen Y, Eastwood M, et al. FAK is required for TGFbeta-induced JNK phosphorylation in fibroblasts: implications for acquisition of a matrix-remodeling phenotype. Mol Biol Cell 2007;18:2169-2178.
15) Mimura Y, Ihn H, Jinnin M, Asano Y, Yamane K, Tamaki K. Constitutive phosphorylation of focal adhesion kinase is involved in the myofibroblast differentiation of scleroderma fibroblasts. J Invest Dermatol 2005;124:886-892.
16) Lagares D, Busnadiego O, Garcia-Fernandez RA, Kapoor M, Liu S, Carter DE, et al. Inhibition of focal adhesion kinase prevents experimental lung fibrosis and myofibroblast formation. Arthritis Rheum 2012;64:1653-1664.
17) Carloni V, Defranco RM, Caligiuri A, Gentilini A, Sciammetta SC, Baldi E, et al. Cell adhesion regulates platelet-derived growth factor-induced MAP kinase and PI-3 kinase activation in stellate cells. Hepatology 2002;36:582-591.
18) Zhao XK, Yu L, Cheng ML, Che P, Lu YY, Zhang Q, et al. Focal adhesion kinase regulates hepatic stellate cell activation and liver fibrosis. Sci Rep 2017;7:4032.
19) Shang N, Arteaga M, Zaidi A, Cotler SJ, Breslin P, Ding X, et al. FAK kinase activity is required for the progression of c-MET/beta-catenin-driven hepataocellular carcinoma. Gene Expr 2016;17: 79-88.
20) Decker NK, Abdelmoneim SS, Yaqoob U, Hendrickson H, Hormes J, Bentley M, et al. Nitric oxide regulates tumor cell cross-talk with stromal cells in the tumor microenvironment of the liver. Am J Pathol 2008;173:1002-1012.
21) Kang N, Yaqoob U, Geng Z, Bloch K, Liu C, Gomez T, et al. Focal adhesion assembly in myofibroblasts fosters a microenvironment that promotes tumor growth. Am J Pathol 2010;177:1888-1900.
22) Liu C, Li J, Xiang X, Guo L, Tu K, Liu Q, et al. PDGF receptor alpha promotes TGF-beta signaling in hepatic stellate cells via transcriptional and post transcriptional regulation of TGF-beta receptors. Am J Physiol Gastrointest Liver Physiol 2014;307:G749-G759.
23) **Dou C**, **Liu Z**, **Tu K**, Zhang H, Chen C, Yaqoob U, et al. P300 acetyltransferase mediates stiffness-induced activation of hepatic stellate cells into tumor-promoting myofibroblasts. Gastroenterology 2018;154:2209-2221.e2214.
24) Mitchell H, Choudhury A, Pagano RE, Leof EB. Ligand-dependent and -independent transforming growth factor-beta

receptor recycling regulated by clathrin-mediated endocytosis and Rab11. Mol Biol Cell 2004;15:4166-4178.
25) Ehrlich M, Shmuely A, Henis YI. A single internalization signal from the di-leucine family is critical for constitutive endocytosis of the type II TGF-beta receptor. J Cell Sci 2001;114:1777-1786.
26) Higuchi M, Kihara R, Okazaki T, Aoki I, Suetsugu S, Gotoh Y. Akt1 promotes focal adhesion disassembly and cell motility through phosphorylation of FAK in growth factor-stimulated cells. J Cell Sci 2013;126:745-755.
27) Wendt MK, Schiemann WP. Therapeutic targeting of the focal adhesion complex prevents oncogenic TGF-beta signaling and metastasis. Breast Cancer Res 2009;11:R68.
28) Lawler S, Feng XH, Chen RH, Maruoka EM, Turck CW, Griswold-Prenner I, et al. The type II transforming growth factor-beta receptor autophosphorylates not only on serine and threonine but also on tyrosine residues. J Biol Chem 1997;272:14850-14859.
29) Hayashida T, Wu MH, Pierce A, Poncelet AC, Varga J, Schnaper HW. MAP-kinase activity necessary for TGFbeta1-stimulated mesangial cell type I collagen expression requires adhesion-dependent phosphorylation of FAK tyrosine 397. J Cell Sci 2007;120:4230-4240.
30) Lagares D, Kapoor M. Targeting focal adhesion kinase in fibrotic diseases. BioDrugs 2013;27:15-23.
31) Galliher AJ, Schiemann WP. Src phosphorylates Tyr284 in TGF-beta type II receptor and regulates TGF-beta stimulation of p38 MAPK during breast cancer cell proliferation and invasion. Cancer Res 2007;67:3752-3758.
32) Hamadi A, Deramaudt TB, Takeda K, Ronde P. Hyper-phosphorylated FAK delocalizes from focal adhesions to membrane ruffles. J Oncol 2010;2010:1-10.
33) Katz BZ, Romer L, Miyamoto S, Volberg T, Matsumoto K, Cukierman E, et al. Targeting membrane-localized focal adhesion kinase to focal adhesions: roles of tyrosine phosphorylation and SRC family kinases. J Biol Chem 2003;278:29115-29120.
34) **Shan J**, **Shen J**, Liu L, Xia F, Xu C, Duan G, et al. Nanog regulates self-renewal of cancer stem cells through the insulin-like growth factor pathway in human hepatocellular carcinoma. Hepatology 2012;56:1004-1014.
35) Xu DD, Wang Y, Zhou PJ, Qin SR, Zhang R, Zhang Y, et al. The IGF2/IGF1R/nanog signaling pathway regulates the proliferation of acute myeloid leukemia stem cells. Front Pharmacol 2018;9:687.
36) Sarkar S, Mirzaei R, Zemp FJ, Wei W, Senger DL, Robbins SM, et al. Activation of NOTCH signaling by tenascin-C promotes growth of human brain tumor-initiating cells. Cancer Res 2017;77:3231-3243.
37) Jiang H, Hegde S, Knolhoff BL, Zhu Y, Herndon JM, Meyer MA, et al. Targeting focal adhesion kinase renders pancreatic cancers responsive to checkpoint immunotherapy. Nat Med 2016;22:851-860.

Author names in bold designate shared co-first authorship.

Supporting Information

Additional Supporting Information may be found at onlinelibrary.wiley.com/doi/10.1002/hep4.1452/suppinfo.